Electronic Supplementary Material (ESI) for Journal of Materials Chemistry A.
This journal is © The Royal Society of Chemistry 2014

Journal Name

Dynamic Article Links ►

Cite this: DOI: 10.1039/c0xx00000x

www.rsc.org/xxxxxx

ARTICLE TYPE

Spray-deposited zinc titanate films obtained via sol-gel synthesis for application in dye-sensitized solar cells

Kuhu Sarkar[a], Erik V. Braden[a], Thomas Fröschl[b], Nicola Hüsing[b] and Peter Müller-Buschbaum*[a,c]

Received (in XXX, XXX) Xth XXXXXXXXX 20XX, Accepted Xth XXXXXXXXX 20XX
DOI: 10.1039/b000000x

Electronic Supplementary Information

S1. Synthesis of zinc titanate films

1.1. Details about the sol-gel route

ZnO sol is prepared as follows: 15 mg/mL of P(S-*b*-EO) solution is prepared in C_3H_7NO (N, N-dimethylformamide) by stirring the mixture at room temperature for 30 minutes. Separately, the desired amount of $Zn(CH_3COO)_2{\cdot}2H_2O$ (ZnO precursor) is dissolved in C_3H_7NO at room temperature as well for 30 minutes. Afterwards, both solutions are filtered individually using 0.45 µm Teflon filters. Then, the required amount of deionized water is added to the filtered polymer solution and the mixture is allowed to stir at room temperature for another 30 minutes (w_{C3H7NO}: w_{H2O}: $w_{Zn(CH3COO)2{\cdot}2H2O}$ = 0.92: 0.005: 0.075). In this course, phase separation of the polymer occurs and micelles are produced in the polymer solution. The rate of micelle formation and the geometry depend on the interaction of the polymer chains with the surrounding solvent environment. Finally, the polymer + C_3H_7NO + H_2O solution and the $Zn(CH_3COO)_2{\cdot}2H_2O$ + C_3H_7NO solution are simultaneously mixed with the aid of a syringe pump, PHD 2000 infuse/withdraw, Harvard Apparatus using a constant infuse rate of 1 mL/min. The final sol is allowed to stir at room temperature for 5 minutes before being used for further processing.

The TiO_2 sol is prepared as follows: P(S-*b*-EO) is dissolved in C_3H_7NO with a concentration of 15 mg/mL by stirring at room temperature for 30 minutes. Once a clear solution is obtained, it is filtered using the Teflon filter and the required amount of HCl is added to the system followed by $Ti(O_2C_2H_4)_2$ (TiO_2 precursor) (w_{C3H7NO}: w_{HCl}: $w_{Ti(O2C2H4)2}$ = 0.905: 0.08125: 0.01375). The mixture is stirred at room temperature for 30 minutes after which a turbid solution is obtained. The temperature of this solution is then raised to 90 °C and the stirring is continued for an additional 15 minutes till a clear pale yellow solution is obtained.

For both sols the weight fraction combinations for the solvent system and the precursors are chosen in a way that the respective sols constitute equal volumes of the precursors. These values are kept constant for all the experiments performed in this study. In order to produce ZnO-TiO_2 composite nanostructures, the above sols are mixed in different volume ratios. However, in order to obtain Zn_2TiO_4 nanostructures in particular, a volume ratio of ZnO sol : TiO_2 sol = 20 : 80 is used. The impact of different mixing ratios on the final film morphology and properties of the nanostructures obtained are discussed in section S 1.3 and S2.

1.2 Comments on the spray parameters and the post-treatment of the films

A custom-made automatized spray setup is used for the deposition of ZnO-TiO_2 nanocomposite films in the present study. One of the biggest advantages of spray deposition technique to obtain nanostructured films for DSSCs, is the scalability of the film thickness. A typical film thickness of 10 – 15 µm is usually favorable for DSSCs to ensure sufficient light absorption, which is easily achieved by spray deposition.[1] All the films discussed here are obtained by multiple spray shots. However, the scaling of the film thickness is not associated linearly with the number of spray shots as each fresh shot dissolves a bit of the underlying layer. The spray deposition technique in principle, involves fast system kinetics and hence the nanostructures obtained are not in equilibrium conditions. However, for many practical applications, the non-equilibrium structures are favorable.[2] The spray geometry employed is shown in Figure 1 (d) of the manuscript. The spray parameters for all the samples studied are kept constant. This includes the pressure of the carrier gas (N_2), which is maintained at 2 bars. The distance between the spray nozzle and the sample surface is kept constant at 16 cm to obtain a homogeneous film. The substrate is kept at 80 °C during spraying. Each spray shot lasts 10 s with a waiting

time of 5 s between two consecutive spray shots. This short waiting time allows the substrate to attain the required temperature before every fresh spray event (as each new spray shot brings fresh solution in contact with the substrate which results in a momentary drop in temperature by 1-2 °C). The nanocomposite films obtained after spraying are annealed at 80 °C.[3] Afterwards, the films are calcined in order to remove the block copolymer template and to obtain crystalline Zn_2TiO_4 nanostructures as mentioned in the experimental section of the manuscript.

1.3 Impact of the ZnO and TiO_2 precursor concentration on the film morphology

sol	conc. ZnO precursor [mol/L]	conc. TiO_2 precursor [mol/L]
I	0.28	0.02
II	0.21	0.03
III	0.07	0.06
IV	0.04	0.08

Table S1. Different combinations of ZnO and TiO_2 precursor concentration used in the final sol for spray deposition of nanostructured films.

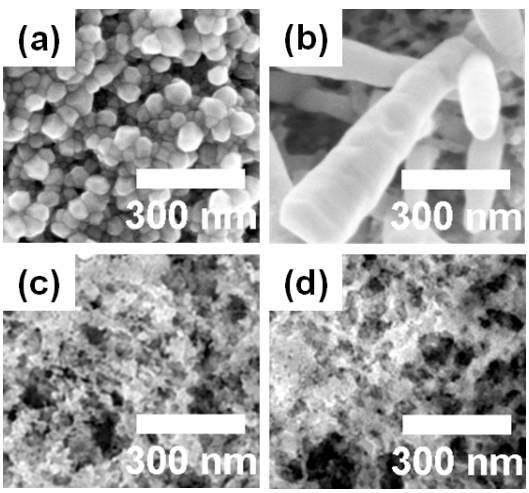

Figure S1. SEM micrographs of calcined nanostructured films obtained by multiple spray coatings. For sols I, II, III and IV (as listed in Table S1), the SEM images of the nanostructures obtained are shown in (a), (b), (c) and (d), respectively.

In order to study the influence of different precursor concentrations on the final film morphology, four sols with different concentration ratios of $Zn(CH_3COO)_2{\cdot}2H_2O$ and $Ti(O_2C_2H_4)_2$ precursors are investigated as listed in Table S1. Figure S1 shows the SEM images of the calcined films obtained by spray deposition of the four different sols. It is clearly seen from the SEM images that the morphologies obtained from sols I (granular) and II (nanorods) are significantly different from that obtained from sols III and IV which essentially show foam-like network morphology. The difference in these morphologies signifies the main essence of the synthesis technique, i.e., multiple morphologies, which might be necessary for different applications, are feasible using a single structure-directing diblock copolymer. It is also important to investigate these different morphologies in terms of their optical properties, which is addressed in the following section.

S2. Characterization of ZnO-TiO_2 nanocomposite films

2.1 Crystallinity investigation

All the four films mentioned in the previous section are characterized by x-ray diffraction technique in order to monitor the crystallinity of the films. Crystallinity is an important parameter for charge transport in photovoltaic systems. The XRD patterns with the corresponding color codes are shown in Figure S2. Interesting properties are revealed by this study, where it is evident that for sols I and II, crystalline ZnO peaks are visible. Whereas, only for the film obtained from sol III, crystalline peaks of Zn_2TiO_4 are achieved. This suggests that the concentration ratios of the precursors in the final sol play an important role in deciding the final composition of the film. The film obtained from sol IV on the other hand, shows low crystallinity. Hence, it is clear that the formation of Zn_2TiO_4 compound is successful via the wet chemical process within a narrow composition range of the final sol. Since, the focus in the present research is on Zn_2TiO_4 phase of ZnO-TiO_2 nanocomposites, the influence of the calcination temperature on the crystallinity is also investigated for the film obtained from sol III. This is presented in the manuscript.

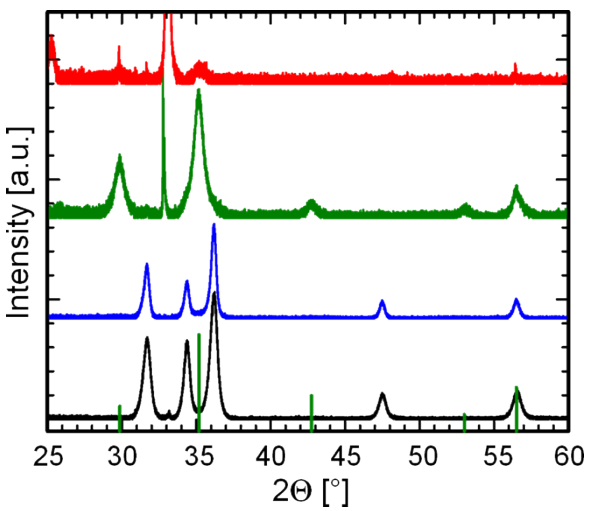

Figure S2. XRD patterns for different sols (I, II, III and IV, from bottom to top as listed in Table S1) with increasing molar concentration of $Ti(O_2C_2H_4)_2$ precursor. The calcination temperature used for these films is 600 °C. All the XRD patterns are shifted along the intensity axis for clarity. The high intensity peak observed at $2\Theta = 33°$ corresponds to the silicon (100) peak originating from the substrate underneath. In order to concentrate more on the peaks obtained from the films, this high intensity peak is cut off at higher intensities. The green vertical lines represent the theoretical peak positions of zinc orthotitanate with their relative intensities.

This journal is © The Royal Society of Chemistry [year]

2.2 Optical characterization – determination of band gap energies

The absorbance spectra for the calcined films obtained from spray deposition of sols I, II, III and IV are shown in Figure S3 (a). As already visible from the spectra, for lower concentrations of $Ti(O_2C_2H_4)_2$ in the solution, i.e., 0.2 and 0.3 mol/L (sols I and II), there are two onsets of absorption visible, denoted by the different slopes of the spectra. These indicate the absence of a single pure phase in the film. However, the absorbance spectra for the films prepared with higher concentrations of $Ti(O_2C_2H_4)_2$, i.e., 0.06 and 0.08 mol/L (sols III and IV), show only a single linear regime which is associated with the presence of a single pure phase in the system. The direct band gap energies extracted for all the films are plotted in Figure S3 (b). Two energies are extracted for different phases in samples I and II (from the different slopes of the absorbance spectra). Between sols III and IV, the band gap energy of sample III is found to lie in the range of reported values for that of Zn_2TiO_4 compound.[4-6] Hence, it can be concluded that pure Zn_2TiO_4 nanostructured film is obtained from sol III.

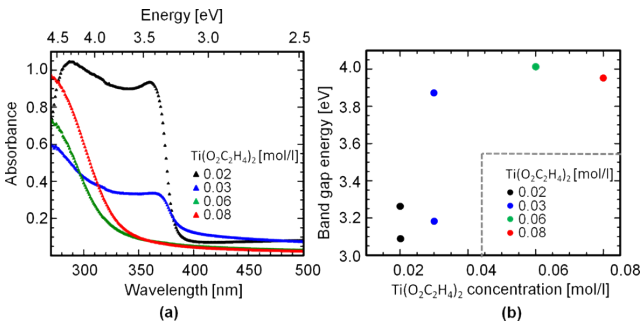

Figure S3. Absorbance spectra and calculated band gaps for spray-deposited ZnO nanostructures. (a) Absorbance spectra of the calcined films obtained after spray deposition of the sols listed in Table S1 with the same color code. (b) The band gaps of the films calculated from the Tauc equation plotted against $Ti(O_2C_2H_4)_2$ concentration in the sol.

2.3 Vertical film composition of the Zn_2TiO_4 film

X-ray reflectivity (XRR) measurements are performed at incidence angle Θ in the range of 0° - 6° with an interval of 0.01°. A typical measurement time of 60 s per step is used. Only specular reflection is detected by the detector and hence, only the z-component of the scattering vector, q_z is probed:

$$q_z = 4\pi\sin(\Theta)/1.54\ \text{Å} \qquad \text{(eq. 1)}$$

The detected signal (shown for Zn_2TiO_4 film in Figure S4 (a)) comprises of interference effects in addition to the Fresnel reflectivity function. The interference fringes are generally damped by the roughness of the film surface. To fit the data, multiple layers are assumed to be present in the film on top of the silicon substrate under ambient atmosphere. For each layer the thickness, the roughness as well as the real and the imaginary parts of the refractive index are fitted individually by an iterative algorithm.[7] The fit to the XRR profile of the Zn_2TiO_4 film is shown in red in Figure S4 (a). The scattering length density profile of the film is obtained from the fit, which is plotted in Figure S4 (b). The porosity of the film is calculated as:

$$\Phi = 1\text{-}(SLD_{film}/SLD_{bulk}) \qquad \text{(eq. 2)}$$

with Φ being the porosity.[8] Using eq. 2, the porosity of the present films is calculated to be (52.5 ± 4.2) %.

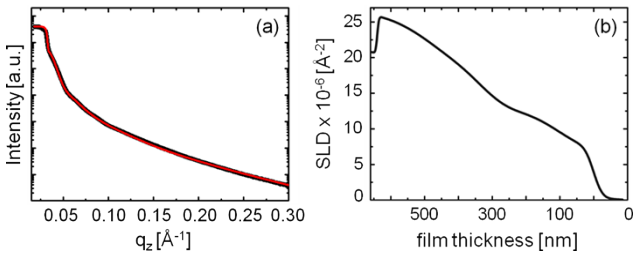

Figure S4. (a) XRR data (black line) with the fit (red line) obtained for the Zn_2TiO_4 foam-like film. (b) SLD profile extracted from the XRR data for the probed thickness of the film.

S3. Dye-sensitized solar cells (DSSCs)

3.1 Scheme for making DSSCs

Fluorine doped tin oxide SnO_2:F (FTO) substrates (Solaronix SA; sheet resistivity =10 $\Omega\square^{-1}$) are first cut in sizes of (2.5 × 2.5) cm^2. In order to clean the substrates, FTOs are treated in an ultrasonic bath successively with Alkonox® detergent (16 g/L) and ethanol for 10 minutes (see Figure S5 (a)). A thin film of pure titania is then deposited on the cleaned FTO substrates via titanium tetrachloride ($TiCl_4$) bath treatment. During this process, the samples are immersed in a 50:1 volume ratio of H_2O:$TiCl_4$ at 70 °C for 45 minutes. Afterwards, the samples are removed and rinsed with H_2O and ethanol respectively (see Figure S5 (b)). The sol solution III (see Table S1 for composition) is then spray-deposited multiple times using the optimized parameters described in section S 1.2 (see Figure S5 (c)). This is followed by a calcination step (as mentioned in the experimental part of the manuscript) to impart crystallinity to the active layer. The samples are allowed to cool down to 80 °C in the furnace, after which they are directly immersed in a 0.5mM solution of dye in 1:1 volume ratio of acetonitrile and 4-tertiary butanol (Sigma Aldrich). The commercial dye is 5-[[4-[4-(2,2-Diphenylethenyl)phenyl]-1,2,3-3a,4,8b-hexahydrocyclopent[b]indol-7-yl]methylene]-2-(3-ethyl-4-oxo-2-thioxo-5- thiazolidinylidene)-4-oxo-3-thiazolidineacetic acid and is commonly abbreviated as D149, is purchased from Sigma Aldrich.[9] The dye soaking time is 1 hour at room temperature (see Figure S5 (d)). After this time, the sample is taken out of the dye and rinsed with ethanol to remove the unadsorbed dye. Most of the film is then scratched away leaving only a defined active area of around 0.15 cm^2 to be measured. A (25 × 20 × 0.1) mm^3 Teflon spacer with a hole of (18 × 12) mm^2 is used as the reservoir for the liquid electrolyte which acts as a redox mediator (see Figure S5 (e)). The Teflon spacer is coated with grease on both sides to prevent leakage of the liquid electrolyte. 250 µL of the liquid electrolyte solution consisting of 0.05 mol/L I2, 0.1 mol/L LiI, 0.6 mol/L 1-butyl-3-methylimidazolium iodide (BMII) and 0.05 mol/L 4-tert-butylpyridine in acetonitrile : valeronitrile (Sigma Aldrich) volume ratio of 85 : 15 is then deposited on the active area (see Figure S5 (f)). The platinum counter electrodes

are prepared by blade coating the commercial platinum paste (PT-1, Dyesol) on cleaned FTOs followed by a temperature treatment at 400 °C for 15 minutes with a heating ramp of 175 °C. The Zn_2TiO_4 layer along with the electrolyte is then sealed with the top Pt electrode in order to obtain the final solar cell as shown in Figure S5 (g). Finally J-V characteristics of the devices are measured as detailed in the experimental part and the power conversion efficiency (PCE) of the devices are calculated using the following equation:

$$PCE = \frac{FF \cdot V_{OC} \cdot J_{SC}}{I_0} \qquad \text{(S1)}$$

where, FF is the fill factor, V_{OC} and J_{SC} denote the open circuit voltage and short circuit current density respectively with I_0 being the illumination intensity.

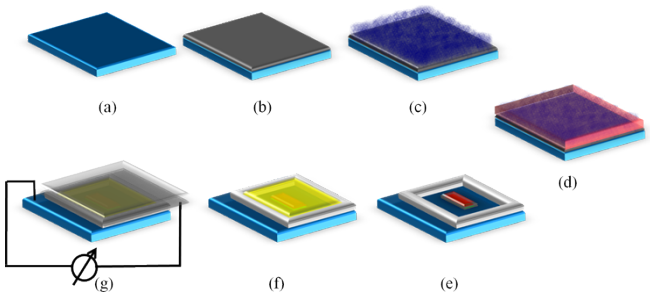

Figure S5. Schematic representation of different steps involved in the fabrication of a dye-sensitized solar cell.

Notes and references S

[a] *Technische Universtität München, Physik-Department, Lehrstuhl für Funktionelle Materialien, James-Franck-Straße 1, 85748 Garching, Germany. Fax: +49 (89) 289-12473; Tel: +49 (89) 289-12451; E-mail: muellerb@ph.tum.de*
[b] *Materialchemie, FB Materialforschung und Physik, Universität Salzburg, Hellbrunnerstraße 34, 5020 Salzburg, Austria*
[c] *Nanosystems Initiative Munich, Schellingstraße 4, 80799 München, Germany*

1 A. Sacco, A. Lamberti, R. Gazia, S. Bianco, D. Manfredi, N. Shahzad, F. Cappelluti, S. Ma and E. Tresso, *Phys. Chem. Chem. Phys.,* 2012, **14,** 16203.
2 A. Abdellah, K. S. Virdi, R. Meier, M. Döblinger, P. Müller-Buschbaum, C. Scheu, P. Lugli and G. Scarpa, *Adv. Funct. Mater.,* 2010, **22**, 4078.
3 M. Rawolle, E. V. Braden, M. A. Niedermeier, D. Magerl, K.Sarkar, T. Fröschl, N. Hüsing, J. Perlich and P. Müller-Buschbaum, *ChemPhysChem,* 2012, **13**, 2412.
4 J. C. Conesa, *Catal. Today,* 2013, **208**, 11.
5 S. A. Mayén-Hernández, G. Torres-Delgado, R. Castanedo-Pérez, M. G. Villarreal, A. Cruz-Orea, J. G. M. Alvarez and O. Zelaya-Angel, *J. Mater. Sci: Mater. Electron.,* 2007, **18**, 1127.
6 C. Wang, B. –Q. Xu, X. Wang and J. Zhao, *J. Solid State Chem.,* 2005, **178**, 3500.
7 L. Paratt, *Phys. Rev*., 1954, **95**, 359.
8 A. Gibaud, S. Dourdain and G. Vignaud, *Appl. Surf. Sci*., 2006, **253**, 3.
9 W-. C. Chang, C-. H. Lee, W-. C. Yu and C-. M. Lin, *Nanoscale Res. Lett.,* 2012, **7**, 688.

This journal is © The Royal Society of Chemistry [year]